HIGH-RESOLUTION SEEDING MONOCHROMATOR DESIGN FOR NGLS*

Yiping Feng, Juhao Wu, Jerome Hastings, SLAC, Menlo Park, CA94025, USA
Paul Emma, Tony Warwick, Robert Schoenlein, LBL, Berkeley, CA 94720, USA

Abstract

A high-resolution soft X-ray monochromator system is designed for self-seeding the next generation FEL sources. It consists of a single variable-line-spacing (VLS) grating, an exit slit, and pre- and collimating mirrors, and operates in the fixed-focus mode to achieve complete tuning of the seeding energy from 200 to 2000 eV with a nearly constant resolving power of greater than 50000, producing transform-limited seed ranging from 1 ps at 200 eV to 100 fs at 2000 eV. The optical delay is of order 1 ps, matching well with that of an electron chicane of moderate magnetic field strength. The design is based on a coherent Gaussian beam treatment of the FEL beam propagating from the upstream SASE undulator through the entire seeding monochromator system, preserving the transverse beam profile entering the downstream seeding undulator to ensure maximum coupling efficiency with the reentrant electron beam.

INTRODUCTION

SASE FEL starts from the shot noise in the electron bunch and is considered to be chaotic, especially in the temporal or spectral domain [1]. This poses limitations for certain user experiments. Schemes such as self-seeding [2] can effectively improve the temporal coherence of the FEL and provide better correlation between the FEL pulse intensity and the peak electric field, which is critically important for X-ray nonlinear physics. If the seeded FEL pulses approach transform-limited, more precise measurement of the pulse duration can be made using spectral methods. Furthermore, the FEL spectral brightness can be greatly enhanced and thus beneficial to experiments where a monochromator is required as in most spectroscopic/resonant excitation measurements. If brought into saturation, a self-seeded FEL pulse will exhibit far more stable intensity, allowing better control of FEL fluence on samples for measurements. Finally a stable self-seeded pulse will enable FEL high-power (at terawatts level) performance with strong tapering, producing even greater X-ray production and higher spectral brightness.

LCLS has commissioned hard X-rays self-seeding (HXRSS) [3] and has been planning for demonstrating soft X-ray self-seeding (SXRSS) with a moderate resolving power of 5000 [4], limiting the transform-limited pulses to 20 fs at 1 keV. Here in this paper, we present the optical design for a high-resolution soft X-ray monochromator system with a resolving power approaching 50000 and complete tunable from 200 to 2000 eV.

* Work supported by US DOE Office of Basic Energy Sciences under Contract DE-AC02-76SF00515 and US DOE Office of Science Early Career Research Program Award FWP-2013-SLAC-100164.

X-RAY OPTICAL DESIGN

The schematic layout of the seeding grating monochromator system is shown in Fig. 1. M_1 is a cylindrical mirror that deflects the beam vertically, but focuses beam horizontally onto the re-entrance point in the seeding undulator. The planar pre-mirror M_2 also deflects the beam vertically. G is a planar variable-line-spacing type [4], which disperses vertically and tunes the seeding energy by varying both the incident and exit angles in conjunction with the rotation of M_2, and focuses the dispersed beam vertically at the exit slit S, whose width is used for selecting the bandwidth. The mirror M_3 re-collimates the monochromatic but divergent beam from the slit S onto the re-entrant point in the seeding undulator to be re-merged with the electron bunch. The specifications of the grating and mirrors are given in Tables 1 and 2, and the system performance is discussed below.

Table 1: Optics Specifications for the Grating

Parameter	Symbol	Value
Line spacing (μm)	σ	0.393
Linear coefficient ()	$\Delta\sigma/\Delta x$	-2.9091 $\times 10^{-7}$
Groove height (nm)	h	5.21
Grating profile		Blazed
Incident angle (mrad)	θ	3.31 - 10.43
Exit angle (mrad)	θ'	56.3 - 178.2
Included angle (degree)	2θ	176.59 - 169.19
Object distance (m)	$L_{\rm obj}$	~ 8.0
Image distance (m)	$L_{\rm img}$	~ 2.7
Exit slit (μm)	s	0.557 - 1.763

Resolving Power

In the current design, the resolving power of a grating is mainly limited by the number of coherently illuminated grating grooves, which is mainly determined by the beam footprint onto the grating at a given incident angle. Since the FEL is nearly fully coherent, and the exit slit width is adjusted to match the size of the image (at the desired resolving power), the source and image size do not contribute to the resolution function. As such, the resolving power is shown in Fig. 2, approaching 50,000 in the entire energy range from 200 to 2,000 eV. In comparison, the LCLS SXRSS system has a resolving power of only 5,000.

ISBN 978-3-95450-126-7

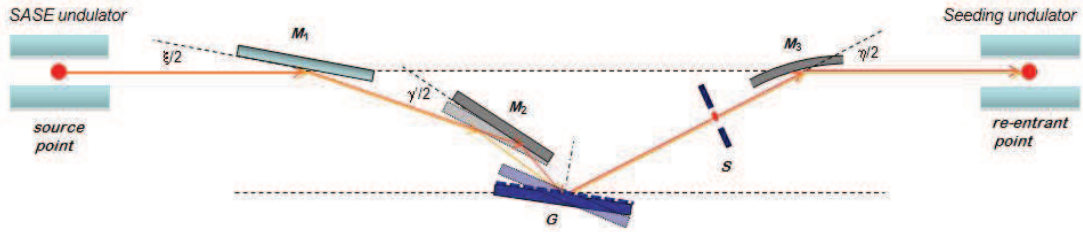

Figure 1: Layout of soft X-ray self-seeding monochromator.

Table 2: Optics Specifications for the Mirrors

Parameter	Symbol	Value
Cylindrical Mirror Radius (m)	R_1	0.0796
Focal length (m)	f_1	7.920
Incident angle (mrad)	$\xi/2$	5.03
Planar Mirror (m)	R_2	∞
Incident angle (mrad)	$\gamma'/2$	21.56 - 86.07
Spherical Mirror Radius (m)	R_3	71.737
focal length (m)	f_3	0.11486
Incident angle (mrad)	$\eta/2$	3.20
Offset-1 (m)	H	0.0180
Offset-2 (m)	H'	0.0162
Offset-3 (mm)	Π	1.778

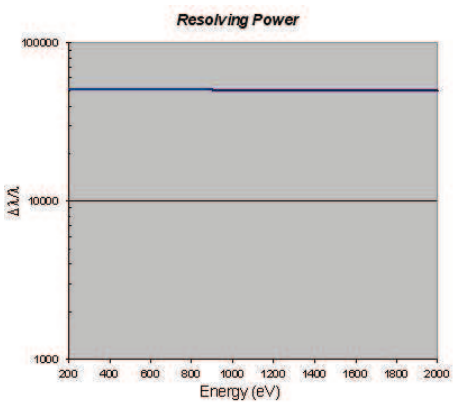

Figure 2: Designed resolving power.

Imaging in the Dispersion Plane

Due to the fact that the SASE FEL develops nearly full transverse coherence, Gaussian optics treatment was necessary to model its propagation through the entire system to help design the correct parameters for the grating and mirrors. The source and image distances are given in Table 3 and depicted in Fig. 3. The Gaussian beam propagation from the source to the exit slit is illustrated in Fig. 4 for the grating G, and from the exit slit to the re-entrant point in Fig. 5 for the collimating mirror M_3. The resulting difference in the image size in the dispersion plane is shown in Fig. 6, where the ray-optics produced a much larger image by a factor of 4 compared that of Gaussian optics.

Table 3: Source and Image Distances of the Grating Monochromator in the Dispersion Plane. The units are mm.

	200 eV	2 keV
L_1	6.384	6.384
L_{M1M2}	1.606	1.575
r_{M2G}	0.010	0.041
r'_{G}	2.698	2.698
r_{M3}	0.115	0.115
r'_{M3}	1.971	1.971
r_{total}	12.784	12.784

Time Delay

The time delay varies with energy because the including angle is not a constant, resulting a path-length difference as the seeding energy is being tuned by rotations of both M_2 and the grating G. This is illustrated in Fig. 7. At the low energy end of 200 eV, the delay $\Delta T \sim 1.036$ ps, with $\delta(\Delta T)/\delta E \sim 1.4$ fs/eV. At the high energy end of 2 keV, the delay $\Delta T \sim 0.653$ ps, with $\delta(\Delta T)/\delta E \sim 0.1$ fs/eV. The results over the energy tuning range in shown in Fig. 8. For practical resonant experiments where tuning of a few eV is needed, this small variation is probably too small to be even measured.

Imaging in the Sagittal Plane

Similar Gaussian beam propagation was done in the Sagittal plane to help define the parameters of mirror M_1 for horizontal focusing onto the re-entrant point. The source and image distances are given in Table 4 and depicted in Fig. 9.

Table 4: Source and Image Distances of the Grating Monochromator in the Sagittal Plane. The units are mm.

	200 eV	2 keV
L_1	6.384	6.384
r'_{M1}	6.401	6.401
r_{total}	12.784	12.784

Grating Efficiency

For the mirrors: M_1, M_2, and M_3 the overall throughput is very close to $\sim$ 100 %. For the grating thee overall

ISBN 978-3-95450-126-7

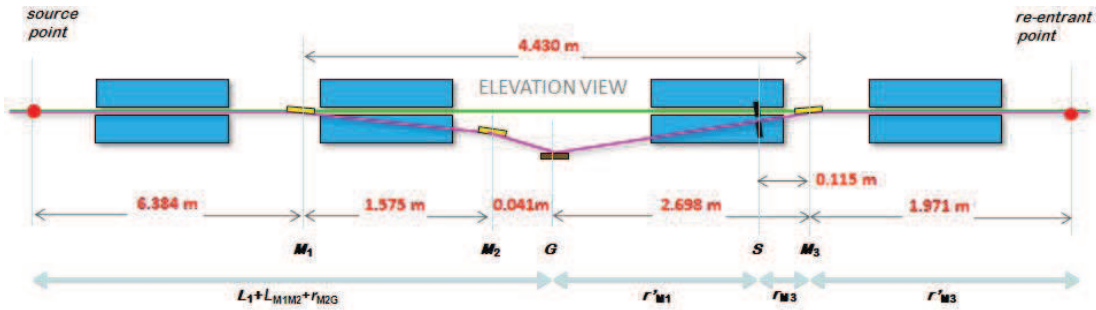

Figure 3: Geometry in the dispersion plane for the soft X-ray self-seeding monochromator.

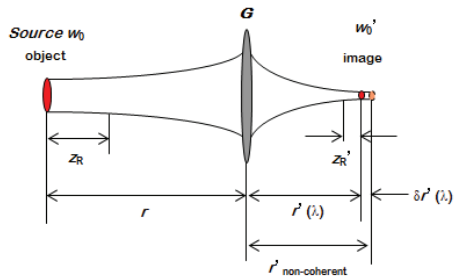

Figure 4: Comparison between coherent mode propagation and ray-optics for grating.

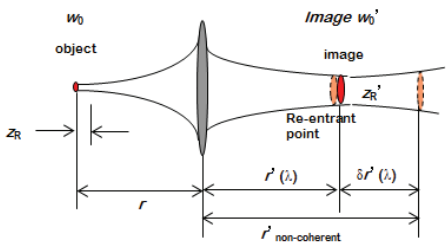

Figure 5: Comparison between coherent mode propagation and ray-optics for M_3.

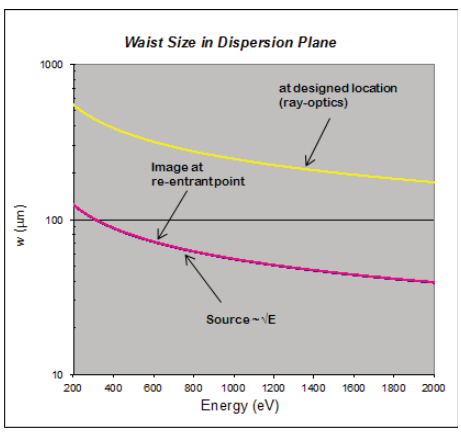

Figure 6: The resulting difference in the waist size between coherent mode propagation and ray-optics.

throughput is about $G \sim R_\lambda \cdot \eta_\lambda \cdot b \sim 0.094\% - 0.023\%$, where $R_\lambda \sim 100\%$ is the reflectivity, η_λ is the estimated grating efficiency, and b is the bandwidth reduction factor. These three factors are shown in Fig. 10. In addition, there will be beam size mismatch effect, but it is very small.

The Seeding Power

The output power will meet the requirement on the seeding power as shown in Fig. 11, there $P_{\rm output} \sim P_{\rm input} \cdot R_\lambda \cdot \eta_\lambda \cdot b$. If on the other hand, considering potential reduced mirror reflectivity, and other reduced efficiency, such as not perfect overlapping between the X-rays and the electron bunch, one might potentially increase the input SASE power going into the monochromator system. This is feasible because the fluence on the mirrors and grating is very below the single-shot damage threshold. For high repetition rate FEL, the optical element will require cooling in order to maintain perfection of the optics for achieving the required resolving power.

Table 5: Optics Specifications for the Mirrors

Parameter	Symbol	Value
Energy range (eV)	ε	200 - 2000
Pulse length (FWHM)	τ	$\sim$ 100
Pulse energy (μJ)	E	2 - 5
Peak Power (MW)	$P_{\rm input}$	20 - 50
e-beam size (FWHM)	s	146 - 46
Resolving power ()	R	$>$ 50000
Throughput (%)	$\eta_{\rm total}$	0.023 - 0.094
Output peak Power (kW)	$P_{\rm output}$	11 - 47
Time delay (ps)	ΔT	0.653 - 1

SUMMARY

Let us now summarize the design specifications for the elements. The grating parameters are in Table 1. The specifications for the mirrors are in Table 2. With these specifications, the overall performance is summarized in Table 5. The design presented in this paper meets all requirements. For the grating monochromator, we choose fixed-focus operation, allowing for tuning the entire energy range with

ISBN 978-3-95450-126-7

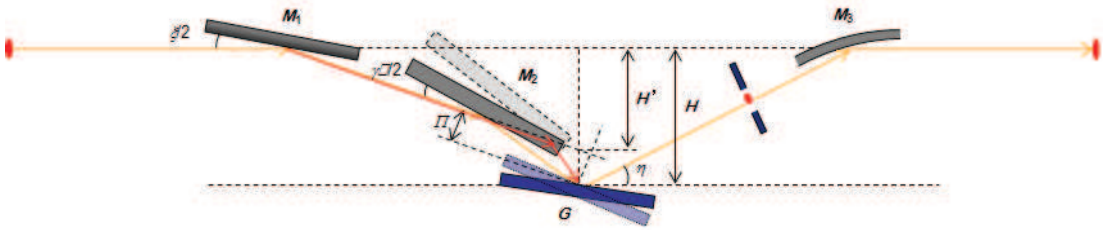

Figure 7: Illustration of the time delay as a function of photo energy.

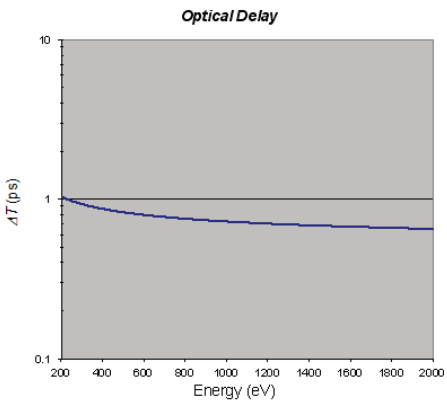

Figure 8: Time delay as a function of FEL photon energy.

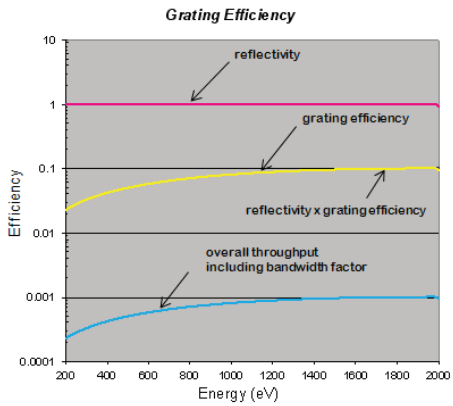

Figure 10: The throughput for the grating.

only a single VLS grating. The overall efficiency is sufficient for seeding. Both estimation and rigorous calculation indicate enough output power after monochromator. Time delay is variable, but is only weakly energy dependent. The imaging properties of the system allow the source point to be nearly perfectly imaged at the re-entrant point, allowing maximum overlap with the re-entrant electron bunch. The high resolving power will allow seeding of much longer electron bunches for enhanced spectral brightness.

REFERENCES

[1] E.L. Saldin *et.al.*, Opt. Comm. **148**, (1998) 383.

[2] J. Feldhaus *et al.*, Opt. Comm. **140**, (1997) 341.

[3] J. Amann *et al.*, Nature Photonics **180**, (2012) 1038.

[4] Y. Feng *et al.*, Proc. FEL'12, Japan, TUOBI01, p. 205 (2012).

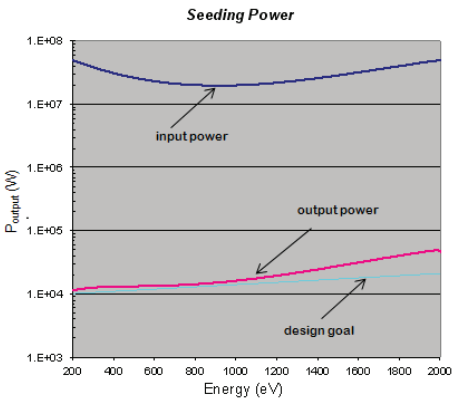

Figure 11: The seeding power.

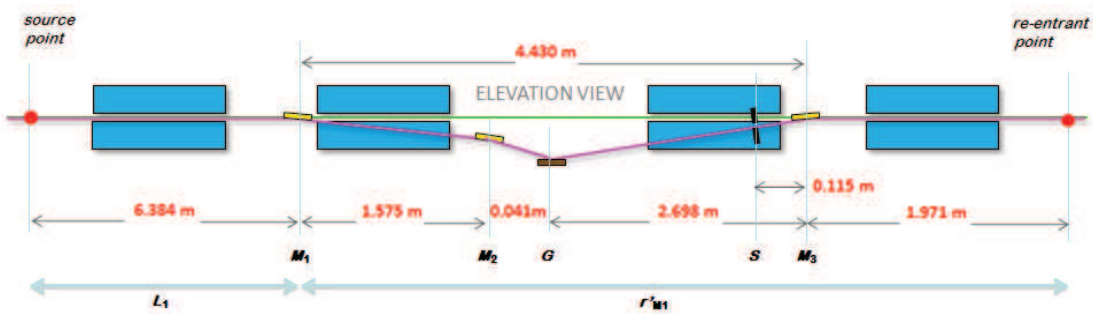

Figure 9: Geometry in the sagittal plane for the soft X-ray self-seeding monochromator.

ISBN 978-3-95450-126-7